

# Wavelet-based Defect Detection System for Grey-level Texture Images

Gintarė Vaidelienė and Jonas Valantinas

*Kaunas University of Technology, Department of Applied Mathematics, Kaunas, Lithuania*

**Keywords:** Texture Images, Defect Detection, Discrete Wavelets Transforms, Statistical Data Analysis, Automatic Visual Inspection.

**Abstract:** In this study, a new wavelet-based approach (system) to the detection of defects in grey-level texture images is presented. This new approach explores space localization properties of the discrete wavelet transform (DWT) and generates statistically-based parameterized defect detection criteria. The introduced system's parameter provides the user with a possibility to control the percentage of both the actually defect-free images detected as defective and/or the actually defective images detected as defect-free, in the class of texture images under investigation. The developed defect detection system was implemented using discrete Haar and Le Gall wavelet transforms. For the experimental part, samples of ceramic tiles, as well as glass samples, taken from real factory environment, were used.

## 1 INTRODUCTION

Visual inspection presents an important part of quality control in manufacturing. Traditionally, product defects are detected by human eyes, but the detection efficiency is low enough because of eye fatigue. Also, the human visual inspection is more or less subjective and highly depends on the experience of human inspectors. Some studies indicate, that an expert, in human visual inspection, typically finds only (60-75) % of the significant defects (Ngan et al., 2011). Therefore, an increased need to develop online visual-based systems capable to enhance not only the quality control but also the marketing of the products is observed.

The defect detection systems are designed and explored for various texture surfaces, such as steel plates, weldment, ceramic tiles, fabric, etc., and are oriented to detect defects like cracks, stains, broken points and other. There are numerous publications offering approaches to solve the problem (Ngan et al., 2011; Karimi et al., 2014; Xie, 2008; Kumar, 2008). Texture defect detection methods can be roughly categorized into four classes (approaches): statistical methods, structural methods, filtering methods and model-based methods.

The statistical approach analyses the spatial distribution values in texture images using various

representations, say, auto-correlation function, co-occurrence matrices, histogram statistics (mean, standard deviation, median, etc.), Weibull distribution (Gururajan et al., 2008; Ghazini et al., 2009; Lin et al., 2007; Latif-Amet et al., 2000; Ivarinent, 2000; Timm et al., 2011), etc.

Filtering methods are based, mainly, on mathematical (linear and non-linear) transforms and on various filtering schemes. In particular, Fourier transform, discrete wavelet transforms, filters (Gabor, Sobel, Gaussian, etc.), neural networks, as well as and genetic algorithms are explored (Han et al., 2007; Ngan et al., 2005; Tsai et al., 2007; Chan et al., 2000; Bissi et al., 2013; Mak et al., 2013; Raheja et al. 2013).

In model-based defect detection approach, a model is selected to analyse the texture image, and the model parameters are desired unknowns. The model-based methods include autoregressive model, Markov random fields, fractal model, etc. Despite the novelty and originality of the ideas employed, the model-based methods have limited areas of application (Bu et al., 2009; Bu et al., 2010; Dogandzic et al., 2005).

The structural approach usually analyses spatial arrangement of texture elements, explores morphological operators and edge detection schemes, hierarchical forms, and often leads to undesirable time-consuming operations. On the other hand, the structural methods perform well with very regular

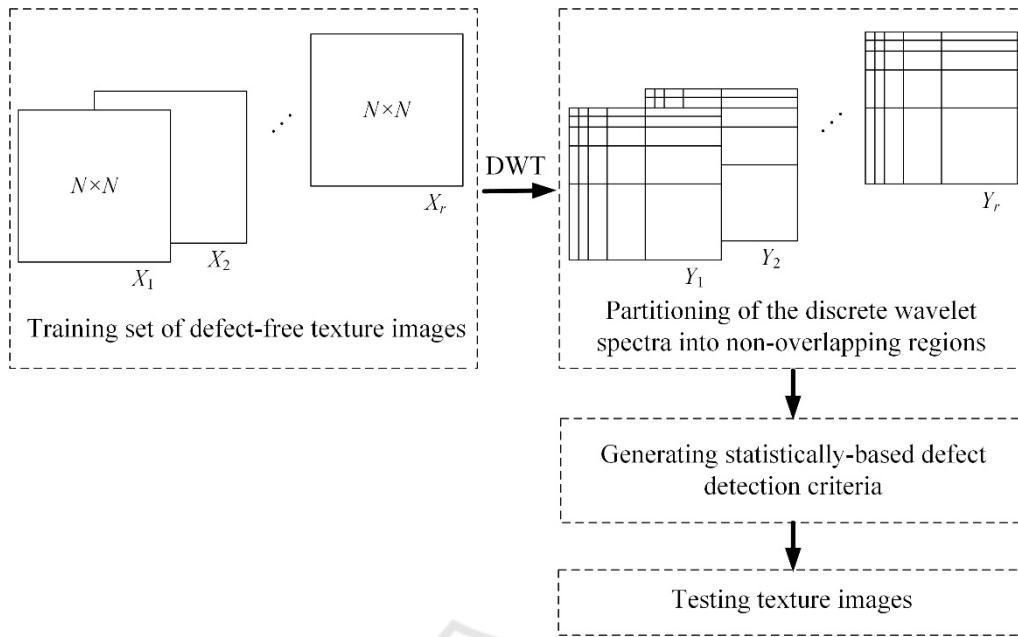


Figure 1: The general scheme of the defect detection system for grey-level texture images.

texture, (Chen et al. 1988; Wen et al., 1999; Mak et al., 2009).

Lately, some hybrid models that combine various ideas mentioned above have appeared (Li et al., 2013; Jia et al., 2014, Yuen et al., 2009; Kim et al., 2006).

In this paper, a novel wavelet-based defect detection system for grey-level texture images is proposed. This system can be used for an automated visual inspection and quality control in a process of serial production, to avoid the financial problems caused by the selling decrements.

## 2 A NEW DEFECT DETECTION SYSTEM FOR TEXTURE IMAGES

The characteristic feature of the proposed defect detection system is simultaneous application of several different scanning filters (two-dimensional wavelets) to the texture image under investigation. The decision on the quality of the test texture image is given depending on a priori prescribed percentage of positive filtering results.

### 2.1 The General Scheme

The general scheme reflecting implementation of the developed defect detection system for grey-level texture images is presented in Fig. 1.

The whole defect detection process comprises five steps, namely (Fig. 1): (1) evaluation of discrete wavelet (DWT) spectra  $Y_j$  for defect-free texture images (contained in the training set)  $X_j$  ( $j=1,2,\dots,r$ ) of size  $N \times N$  ( $N=2^n$ ,  $n \in \mathbb{N}$ ); (2) task-oriented partitioning of the discrete DWT spectrum  $Y_j$  ( $j \in \{1,2,\dots,r\}$ ) into a finite number of non-overlapping regions  $\mathfrak{R}(i_1, i_2)$  ( $i_1, i_2 = 0, 1, \dots, n$ ); (3) statistical analysis of wavelet coefficients falling into a particular region  $\mathfrak{R}(i_1, i_2)$  ( $i_1, i_2 \in \{0, 1, \dots, n\}$ ); (4) generation of parameterized defect detection criteria (sigma intervals)  $I_p = I_p(i_1, i_2)$ , for all regions  $\mathfrak{R}(i_1, i_2)$  ( $i_1, i_2 = 0, 1, \dots, n$ ;  $p \in [0.10, 0.99]$ ); (5) testing a texture image  $X_{test}$ .

### 2.2 Partitioning of the Discrete Wavelet Spectrum of an Image

Consider a texture image  $X = [X(m_1, m_2)]$  ( $m_1, m_2 \in \{0, 1, \dots, N-1\}$ ,  $N=2^n$ ,  $n \in \mathbb{N}$ ). Let  $Y = [Y(k_1, k_2)]$  ( $k_1, k_2 \in \{0, 1, \dots, N-1\}$ ) be its two-dimensional discrete wavelet (DWT) spectrum.

The partitioning of the DWT spectrum  $Y = [Y(k_1, k_2)]$  into a finite number of non-intersecting subsets (regions)  $\mathfrak{R}(i_1, i_2)$

$(i_1, i_2 \in \{0, 1, \dots, n\})$  is based on the following two observations, namely (Fig. 2):

1. Indices  $k_1$  and/or  $k_2$  of any wavelet coefficient  $Y(k_1, 0)$ ,  $Y(0, k_2)$  or  $Y(k_1, k_2)$  ( $k_1, k_2 \in \{1, 2, \dots, N-1\}$ ), can be uniquely represented in the form  $k_1 = 2^{n-i_1} + j_1$ ,  $k_2 = 2^{n-i_2} + j_2$ , where  $i_1, i_2 \in \{1, 2, \dots, n\}$ ,  $j_1 \in \{0, 1, \dots, 2^{n-i_1} - 1\}$  and  $j_2 \in \{0, 1, \dots, 2^{n-i_2} - 1\}$ .

2. The numerical values of all wavelet coefficients, falling into a particular region,  $\mathfrak{R}(0, 0)$ ,  $\mathfrak{R}(i_1, 0)$ ,  $\mathfrak{R}(0, i_2)$  or  $\mathfrak{R}(i_1, i_2)$  ( $i_1, i_2 \in \{1, 2, \dots, n\}$ ), are specified by pixel values of image blocks of size  $2^n \times 2^n$ ,  $2^{i_1} \times 2^n$ ,  $2^n \times 2^{i_2}$  and  $2^{i_1} \times 2^{i_2}$ , respectively. The latter image blocks cover the whole texture image  $X$ . Also, for Haar wavelets, these smaller image blocks do not overlap, whereas for higher order wavelets (Le Gall, Daubechies D4, etc. (Valantinas et al., 2013)) partial overlapping is observed.

		$k_2$			
		0	1	2	3
		$i_2 = 2$		$i_2 = 1$	
$k_1$	0	$\mathfrak{R}(0, 0)$	$\mathfrak{R}(0, 2)$	$\mathfrak{R}(0, 1)$	
---					
$i_1 = 2$	1	$\mathfrak{R}(2, 0)$	$\mathfrak{R}(2, 2)$	$\mathfrak{R}(2, 1)$	
---					
2					
$i_1 = 1$	3	$\mathfrak{R}(1, 0)$	$\mathfrak{R}(1, 2)$	$\mathfrak{R}(1, 1)$	
---					
3					

Figure 2: Partitioning of the DWT spectrum  $Y$  into a finite number of non-intersecting regions ( $N = 4$ ).

### 2.3 Generating Statistically-based Defect Detection Criteria

Suppose,  $\{X_1, X_2, \dots, X_r\}$  is a collection (training set) of good samples, randomly selected from some total population  $X$  of defect-free texture images of size  $N \times N$  ( $N = 2^n$ ,  $n \in \mathbb{N}$ ), and  $\{Y_1, Y_2, \dots, Y_r\}$  is the corresponding set of their DWT spectra. In implementing defect detection criteria for texture images, the following algorithmic steps are performed:

1. For all  $s = 1, 2, \dots, r$ , the averaged values of

wavelet coefficients, falling into the regions  $\mathfrak{R}(i_1, i_2)$  ( $i_1, i_2 \in \{0, 1, \dots, n\}$ ), are found:

$$\bar{Y}_s(0, 0) = |Y_s(0, 0)|$$

$$\bar{Y}_s(i_1, 0) = \frac{1}{2^{2n-i_1}} \sum_{j_1=0}^{2^{n-i_1}-1} |Y_s(k_1, 0)|$$

$$\bar{Y}_s(0, i_2) = \frac{1}{2^{2n-i_2}} \sum_{j_2=0}^{2^{n-i_2}-1} |Y_s(0, k_2)|$$

$$\bar{Y}_s(i_1, i_2) = \frac{1}{2^{2n-i_1-i_2}} \sum_{j_2=0}^{2^{n-i_2}-1} \sum_{j_1=0}^{2^{n-i_1}-1} |Y_s(k_1, k_2)|.$$

2. For each region  $\mathfrak{R}(i_1, i_2)$  ( $i_1, i_2 = 0, 1, \dots, n$ ), using sample values  $(\bar{Y}_1(i_1, i_2), \bar{Y}_2(i_1, i_2), \dots, \bar{Y}_r(i_1, i_2))$ ,

and applying the statistical analysis methods, the statistical hypothesis on the type of the distribution (normal, lognormal, exponential, etc.) of the mean value (random variable)  $\bar{Y}(i_1, i_2)$ , representing precisely the same region of the total population  $X$ , is tested.

3. Depending on the type of the distribution of the mean value  $\bar{Y}(i_1, i_2)$  ( $i_1, i_2 \in \{0, 1, \dots, n\}$ ) and a priori prescribed probability  $p$  ( $p \in [0.10, 0.99]$ ), the corresponding sigma interval  $I_p = I_p(i_1, i_2)$  is found, namely: (1) for the normal distribution ( $\bar{Y} \sim N(m, \sigma)$ ),  $I_p = (m - t \cdot \sigma, m + t \cdot \sigma)$ , where  $t = \Phi_0^{-1}(p/2)$  and  $\Phi_0(t)$  is the Laplace function; (2) for the lognormal distribution ( $\bar{Y} \sim \ln N(m, \sigma)$ ),  $I_p = (m/\sigma^t, m \cdot \sigma^t)$ , where  $t = \Phi_0^{-1}(p/2)$ ; (3) for the exponential distribution ( $\bar{Y} \sim E(\lambda)$ ),  $I_p = [0, t \cdot \sigma)$ , where  $t = -\ln(1-p)$  and  $\sigma = 1/\lambda$ .

### 2.4 Testing Texture Images

Let  $X_{test}$  be a test texture image of size  $N \times N$  ( $N = 2^n$ ,  $n \in \mathbb{N}$ ). Let  $Y_{test}$  be its discrete wavelet (DWT) spectrum. This spectrum is partitioned into a finite number of non-intersecting regions  $\mathfrak{R}(i_1, i_2)$  ( $i_1, i_2 = 0, 1, \dots, n$ ), and the mean values  $\bar{Y}_{test}(i_1, i_2)$  of wavelet coefficients, falling into  $\mathfrak{R}(i_1, i_2)$ , are calculated.

Taking into consideration a priori prescribed value of the system's parameter (probability)  $p$ , the defect detection criteria (sigma intervals)  $I_p = I_p(i_1, i_2)$  ( $i_1, i_2 = 0, 1, \dots, n$ ) are selected.

The test image  $X_{test}$  is assumed to be defect-free, provided the number of mean values  $\bar{Y}_{test}(i_1, i_2)$  ( $i_1, i_2 \in \{0, 1, \dots, n\}$ ), falling into the respective sigma intervals  $I_p(i_1, i_2)$ , is not less than  $p(n+1)^2$ . Otherwise,  $X_{test}$  is assumed to be defective.

By selecting the value of  $p$ , we are given a possibility to control the risk boundary, i.e. we can increase (decrease) the percentage of actually defect-free images detected as defective or that of actually defective images detected as defect-free).

The overall performance of the proposed defect detection system can be improved by exploring only a properly chosen subset of sigma intervals  $I_p = I_p(i_1, i_2)$  ( $i_1, i_2 = 0, 1, \dots, n$ ). Say, if some grid-lines are visible in texture images, the usage of intervals  $I_p = I_p(i_1, i_2)$ , with  $i_1, i_2 \in \{0, m, m+1, \dots, n\}$  ( $1 < m \leq n$ ), may serve the purpose because it excludes comparison of less than  $2^m$  neighbouring pixels of the texture image, in both the vertical and the horizontal directions.

### 3 EXPERIMENTAL ANALYSIS RESULTS AND DISCUSSION

To evaluate performance of the proposed texture defect detection system, two sets of texture images, taken from factories of Lithuania, have been selected and processed, namely: defect-free glass sheet images

of size  $256 \times 256$  (100 samples; Fig. 3, a) and defective glass sheet images of the same size (100 samples; Fig. 3, b), as well as ceramic tile images of size  $256 \times 256$  (100 defect-free samples and 100 defective samples; Fig. 4).

All experiments have been implemented on a personal computer using MatLab. Computer simulation was performed on a PC with CPU Intel Core i5-4200 U CPU@2.36Hz, 8GB of memory.

The statistically-based texture defect detection criteria have been prepared and presented in both the Haar and the Le Gall wavelet domains.

For each class of texture images, five experiments were carried out. For each experiment, 50 defect-free texture images (out of 100) and 50 defective texture images (out of 100) were selected at random. Experimental analysis results are presented in Table 1 (glass sheet images) and Table 2 (ceramic tile images), where: TP – the percentage of actually defective images detected as defective; FP – the percentage of actually defect-free images detected as defective; TN – the percentage of actually defect-free images detected as defect-free; FN – the percentage of actually defective images detected as defect-free.

To summarize the results obtained, i.e. to evaluate performance of the proposed texture defect detection system (Section 2), some secondary system's performance parameters, widely used in this area, were introduced, namely: Specificity =  $TN / (TN + FP)$ , Sensitivity =  $TP / (TP + FN)$  and Accuracy =  $(TP + TN) / (TP + TN + FP + FN)$ .

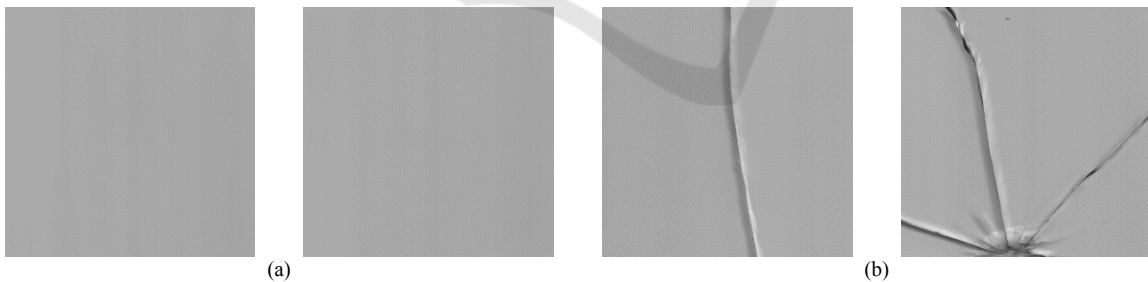


Figure 3: Glass sheet samples: (a) defect-free images; (b) defective images.

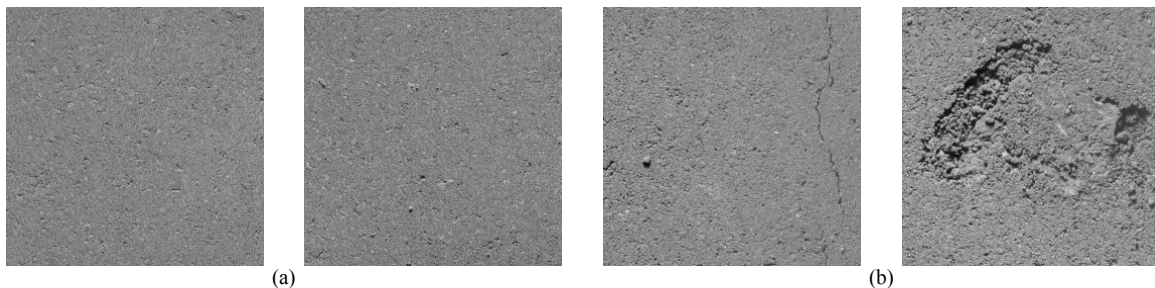


Figure 4: Ceramic tile samples: (a) defect-free images; (b) defective images.

Table 1: Glass sheet classification results using discrete Haar and Le Gall wavelet transforms.

Probability, $p$		Discrete Haar wavelet transform (percentage)					Discrete Le Gall wavelet transform (percentage)				
		Exp. 1	Exp. 2	Exp. 3	Exp. 4	Exp. 5	Exp. 1	Exp. 2	Exp. 3	Exp. 4	Exp. 5
0.99	TP	100	100	98	98	96	96	92	92	96	92
	FP	2	0	2	4	2	42	38	42	40	38
	TN	98	100	98	96	98	58	62	58	60	62
	FN	0	0	2	2	4	4	8	8	4	8
0.95	TP	100	100	98	98	96	96	90	88	94	86
	FP	8	6	8	8	6	42	36	40	36	36
	TN	92	94	92	92	94	58	64	60	64	64
	FN	0	0	2	2	4	4	10	12	6	14
0.90	TP	100	100	98	98	96	86	80	86	84	82
	FP	14	14	12	16	10	44	36	34	36	30
	TN	86	86	88	84	90	56	64	66	64	70
	FN	0	0	2	2	4	14	20	14	16	18

Table 2: Ceramic tile classification results using discrete Haar and Le Gall wavelet transforms.

Probability, $p$		Discrete Haar wavelet transform (percentage)					Discrete Le Gall wavelet transform (percentage)				
		Exp. 1	Exp. 2	Exp. 3	Exp. 4	Exp. 5	Exp. 1	Exp. 2	Exp. 3	Exp. 4	Exp. 5
0.99	TP	100	98	96	98	100	98	96	100	96	98
	FP	2	2	8	4	2	26	16	16	22	22
	TN	98	98	92	96	98	74	84	84	78	78
	FN	0	2	4	2	0	2	4	0	4	2
0.95	TP	98	98	96	96	100	100	98	100	98	98
	FP	2	0	10	4	6	38	36	36	40	44
	TN	98	100	90	96	94	62	64	64	60	56
	FN	2	2	4	4	0	0	2	0	2	2
0.90	TP	96	90	94	96	100	100	98	100	98	98
	FP	4	6	10	6	6	40	34	34	38	40
	TN	96	94	90	94	94	60	66	66	62	60
	FN	4	10	6	4	0	0	2	0	2	2

Table 3: Performance of the defect detection system,  $p = 0.99$ .

Test image	Discrete Haar wavelet domain			Discrete Le Gall wavelet domain		
	Specificity	Sensitivity	Accuracy	Specificity	Sensitivity	Accuracy
Glass sheets	0.98	0.98	0.98	0.60	0.94	0.77
Ceramic tiles	0.97	0.98	0.96	0.80	0.98	0.89

Table 4: Performance of the defect detection system,  $p = 0.95$ .

Test image	Discrete Haar wavelet domain			Discrete Le Gall wavelet domain		
	Specificity	Sensitivity	Accuracy	Specificity	Sensitivity	Accuracy
Glass sheets	0.93	0.98	0.96	0.62	0.91	0.76
Ceramic tiles	0.97	0.98	0.96	0.61	0.99	0.80

Table 5: Performance of the defect detection system,  $p = 0.90$ .

Test image	Discrete Haar wavelet domain			Discrete Le Gall wavelet domain		
	Specificity	Sensitivity	Accuracy	Specificity	Sensitivity	Accuracy
Glass sheets	0.87	0.98	0.93	0.64	0.84	0.74
Ceramic tiles	0.94	0.95	0.94	0.63	0.99	0.81

The averaged values of the above secondary performance parameters (covering all five experiments), for both classes of texture images, are presented in Tables 3, 4 and 5.

First of all, we notice that (Tables 3, 4 and 5), nearly for all indicated values of the probability  $p$ ,

the Haar wavelets perform better than the Le Gall wavelets. The only exception, the sensitivity values for the class of ceramic tiles: 0.98, for  $p = 0.99$ , and 0.99, for  $p \in \{0.90, 0.95\}$ . So, Le Gall wavelets should be explored if one is interested in the selection of high quality products (ceramic tiles), i.e. in

eliminating all defective tiles, even at the expense of some defect-free tiles.

Secondly, let us observe that comparison of the above results with analogous results obtained using other approaches and other texture defect detection schemes is complicated enough. The necessary precondition is to use the same texture image databases. Otherwise, the comparison is not impartial.

Despite this fact, some parallels can be drawn. For instance, in reference (Jin et al., 2011), we found that the glass defect inspection technology based on Dual CCFL performs with success rate (accuracy) 0.99. In (Zhao et al., 2012), the task-oriented application of digital image processing leads to the averaged accuracy 0.916, in the same class of texture images. Segmentation-based classification of pavement tiles (Nguyen et al., 2011) gives the accuracy 0.93. In (de Andrade et. al., 2011), the authors explore infrared images and artificial neural network, and the overall accuracy is 0.926.

In connection with this, we here emphasize that the texture defect detection rate (accuracy), obtained in our experiments using discrete Haar wavelets, are comparatively high, what allows us to state that the developed defect detection system is worth attention and can contribute to improving automated texture inspection schemes in industry.

## 4 CONCLUSIONS

In this paper, a new wavelet-based defect detection system for texture images is proposed. The proposed system explores space localization properties of the discrete wavelet (Haar, Le Gall, etc.) transform, generates statistically-based texture defect detection criteria and leaves space for controlling the risk.

The experimental analysis results, demonstrating the use of the developed defect detection system for the visual inspection of glass sheets, as well as ceramic tiles, obtained from real factory environment, showed that the averaged defect detection rate (accuracy) of the system was high enough: 0.98 for glass sheets, and 0.96, for ceramic tiles, provided the discrete Haar wavelets are employed and the system's parameter  $p = 0.99$ .

Based on our own experience, we here emphasize that, for a particular class of texture images, diligent and serious adaptation of the developed defect detection system is necessary. In each case, not only numerical values of the parameter  $p$  but also various task-oriented subsets of sigma intervals should be looked through carefully.

Also, let us mention that the proposed defect detection system has been applied to the inspection of fabric scraps (textile images). The achieved defect detection success rate (accuracy), on average, turned out to be quite acceptable, i.e. 0.931 (Haar wavelet domain), for  $p = 0.975$  (Vaidelienė et al., 2016).

Our nearest future work will focus on the analysis of the potential relationship between the mathematical measures (coarseness, directionality, etc.), used to classify a given texture, and the choice of the most appropriate subset of sigma intervals, comprising the defect detection criterion (Section 2), for the same texture. In parallels, we are to analyse possibility and efficiency of the application of higher order statistics (e.g. sample variance) to developing wavelet-based texture defect detection criteria.

## REFERENCES

- Bissi, L., Baruffa, G., Placidi, P., Ricci, E., Scorzoni, A., 2013. Automated defect detection in uniform and structured fabrics using Gabor filters and PCA. *Journal of Visual Communication and Image Representation*, 24, 838-845.
- Bu, H. G., Wang, J., Huang, X. B., 2009. Fabric defect detection based on multiple fractal features and support vector data description. *Engineering Applications of Artificial Intelligence*, 22(2), 224-235.
- Bu, H.-G., Huang, X.-B., Wang, J., Chen, X., 2010. Detection of fabric defects by auto-regressive spectral analysis and support vector data description. *Textile Research Journal*, 80(7), 579-589.
- Chan, C., Pang, G., 2000. Fabric defect detection by Fourier analysis. *IEEE Transactions on Industry Applications*, 36(5), 1267-1276.
- Chen, J., Jain, A. K., 1988. A structural approach to identify defects in textural images. In *Proceedings of IEEE International Conference on Systems, Man and Cybernetics, Beijing*.
- de Andrade, R. M., Eduardo, A. C., 2011. Methodology for automatic process of the fired ceramic tile's internal defect using ir images and artificial neural network. *Journal of the Brazilian Society of Mechanical Sciences and Engineering*, 33(1), 67-73.
- Dogandzic, A., Eua-anant, N., Zhang, B. H., 2005. Defect detection using hidden Markov random fields. In *AIP Conference Proceedings*, 760, 704-711.
- Ghazini, M., Monadjemi, A., Jamshidi, K., 2009. Defect detection of tiles using 2D wavelet transform and statistical features. *International Journal of Electrical, Computer, Energetic, Electronic and Communication Engineering*, 3(1), 89-92.
- Gururajan, A., Sari-Sarraf, H., Hequet, E. F., 2008. Statistical approach to unsupervised defect detection and multiscale localization in two texture images. *Optical Engineering*, 47(2).

- Han, Y., Shi, P., 2007. An adaptive level-selecting wavelet transform for texture defect detection. *Image and Vision Computing*, 25, 1239-1248.
- Iivarinen, J., 2000. Surface defect detection with histogram-based texture features. In *Proc. SPIE 4197, Intelligent Robots and Computer Vision XIX: Algorithms, Techniques, and Active Vision*.
- Jia, H. B., Murphey, Y. L., Shi, J. J., Chang, T. S., 2014. An intelligent real-time vision system for surface defect detection. In *Proceedings of the 17th International Conference on Pattern Recognition*, 239-242.
- Jin, Y., Wang, Z. B., Zhu, L. Q., Yang, J. L., 2011. Research on in-line glass defect inspection technology based on Dual CCFL. *Procedia Engineering*, 15, 1797-1801.
- Karimi, M. H., Asemani, D., 2014. Surface defect detection in tiling industries using digital image processing methods: Analysis and evaluation. *ISA Transactions*, 53, 834-844.
- Kim, S. C., Kang, T. J., 2006. Automated defect detection system using wavelet packet frame and Gaussian mixture model. *Journal of the Optical Society of America A-Optics Image Science and Vision*, 23(11), 2690-2701.
- Kumar, A., 2008. Computer-vision-based fabric defect detection: a survey. *IEEE Transactions on Industrial Electronics*, 55(1), 348-363.
- Latif-Amet, A., Ertüzün, A., Erçil, A., 2000. An efficient method for texture defect detection: sub-band domain co-occurrence matrices. *Image and Vision Computing*, 18, 543-553.
- Li, Y. D., Ai, J. X., Sun C. Q., 2013. Online fabric defect inspection using smart visual sensors. *Sensors*, 13(4), 4659-4673.
- Lin, H. D., 2007. Automated visual inspection of ripple defects using wavelet characteristic based multivariate statistical approach. *Image and Vision Computing*, 25(11), 1785-1801.
- Mak, K. L., Peng, P., Yiu, K. F. C., 2009. Fabric defect detection using morphological filters. *Image and Vision Computing*, 27, 1585-1592.
- Mak, K. L., Peng, P., Yiu, K. F. C., 2013. Fabric defect detection using multi-level tuned-matched Gabor filters. *Journal of Industrial and Management Optimization*, 8(2), 325-341.
- Ngan, H. Y. T., Pang, G. K. H., Yung, N. H. C., 2011. Automated fabric defect detection - A review. *Image and Vision Computing*, 29, 442-458.
- Ngan, H. Y. T., Pang, G. K. H., Yung, N. H. C., Ng, M. K., 2005. Wavelet based methods on patterned fabric defect detection. *Pattern Recognition*, 38, 559-576.
- Nguyen, T. S., Begot, S., Duculty, F., Avila, M., 2011. Free-form anisotropy: a new method for crack detection on pavement surface images. In *18th IEEE International Conference on Image Processing*.
- Raheja, J. L., Kumar, S., Chaudhary, A., 2013. Fabric defect detection based on GLCM and Gabor filter: a comparison. *Journal for Light and Electron Optics*, 124, 6469-6474.
- Timm, F., Barth, E., 2011. Non-parametric texture defect detection using Weibull features. In *Proc. SPIE 7877, Image Processing: Machine Vision Applications*.
- Tsai, D. M., Kuo, C. C., 2007. Defect detection in inhomogeneously textured sputtered surfaces using 3D Fourier image reconstruction. *Machine Vision and Applications*, 18(6), 383-400.
- Vaideliënė, G., Valantinas, J., Ražanskas, P., 2016 (to appear). On the use of discrete wavelets in implementing controllable defect detection system for texture images. *Information Technology and Control*.
- Valantinas, J., Kančelkis, D., Valantinas, R., Viščiūtė, G., 2013. Improving space localization properties of the discrete wavelet transform. *Informatica*, 24(4), 657-674.
- Wen, W., Xia, A., 1999. Verifying edges for visual inspection purposes. *Pattern Recognition Letters*, 20, 315-328.
- Xie, X., 2008. Review of recent advances in surface defect detection using texture analysis techniques. *Electronic Letters on Computer Vision and Image Analysis*, 7(3), 1-22.
- Yuen, C. W. M., Wong, W. K., Qian, S. Q., Chan, L. K., Fung, E. H. K., 2009. A hybrid model using genetic algorithm and neural network for classifying garment defects. *Expert Systems with Applications*, 36, 2037-2047.
- Zhao, X. F., Yang, J., Zhang, G. B., 2012. Glass defect detection based on image processing. In *4th International Conference on Software Technology and Engineering*, 155-159.